Available online at www.sciencedirect.com
ScienceDirect
Geotextiles and Geomembranes 26 (2008) 239–249
Geotextiles and Geomembranes
www.elsevier.com/locate/geotexmem

Combined effect of PVDs and reinforcement on embankments over rate-sensitive soils

R. Kerry Rowe*, C. Taechakumthorn

Department of Civil Engineering, GeoEngineering Centre at Queen's-RMC, Queen's University, Canada

Received 27 August 2007; received in revised form 13 October 2007; accepted 15 October 2007
Available online 26 November 2007

Abstract

A numerical study of the behavior of geosynthetic-reinforced embankments constructed on soft rate-sensitive soil with and without prefabricated vertical drains (PVDs) is described. The time-dependent stress–strain-strength characteristic of rate-sensitive soil is taken into account using an elasto-viscoplastic constitutive model. The effects of reinforcement stiffness, construction rate, soil viscosity as well as PVD spacing are examined both during and following construction. A sensitivity analysis shows the effect of construction rate and PVD spacing on the short-term and long-term stability of reinforced embankments and the mobilized reinforcement strain. For rate-sensitive soils, the critical period with respect to the stability of the embankment occurs after the end of the construction due to a delayed, creep-induced, build-up of excess pore pressure in the viscous foundation soil. PVDs substantially reduce the effect of creep-induced excess pore pressure, and hence not only allow a faster rate of consolidation but also improve the long-term stability of the reinforced embankment. Furthermore, PVDs work together with geosynthetic reinforcement to minimize the differential settlement and lateral deformation of the foundation. The combined use of the geosynthetic reinforcement and PVDs enhances embankment performance substantially more than the use of either method of soil improvement alone.

Keywords: Elasto-viscoplastic; Prefabricated vertical drains; Reinforced embankment; Numerical modeling; Time-dependent behavior; Rate-sensitive clay

1. Introduction

Several techniques have been developed for the safe and cost-effective construction of embankments over soft soil deposits. Two of particular note are the use of geosynthetic basal reinforcement (Rowe, 1984; Fowler and Koerner, 1987; Jewell, 1987; Rowe and Soderman, 1987; Rowe and Li, 1999; Bergado et al., 2002b; Shen et al., 2005; Varuso et al., 2005; Bergado and Teerawattanasuk, 2008; Rowe and Taechakumthorn, 2007a; Kelln et al., 2007) and prefabricated vertical drains, PVDs (Crawford et al., 1992; Chai and Miura, 1999; Li and Rowe, 1999; Indraratna and Redana, 2000; Zhu and Yin, 2001, 2004; Bergado et al., 2002a; Bo, 2004; Chai et al., 2004, 2006; Nagahara et al., 2004; Shen et al., 2005; Rujikiatkamjorn et al., 2007; Sinha et al., 2007). The combined use of geosynthetic reinforcement and PVDs has been shown to potentially allow the rapid construction of a higher embankment on rate-insensitive soils that can be achieved with the use of either method alone (Li and Rowe, 2001). However, to date, there has been a paucity of research into the combined effects for embankments constructed on rate-sensitive soils.

The behavior of rate-sensitive soil has been extensively studied (Lo and Morin, 1972; Vaid and Campanella, 1977; Vaid et al., 1979; Graham et al., 1983; Kabbaj et al., 1988; Leroueil, 1988). The performance of the reinforced embankment constructed on the rate-sensitive soil also has been investigated by both field studies and numerical analysis (Rowe et al., 1995, 1996; Hinchberger and Rowe, 1998; Rowe and Hinchberger, 1998; Rowe and Li, 2002; Rowe and Taechakumthorn, 2007a). For example, Rowe et al. (1996) showed that in order to accurately predict the responses of the Sackville test embankment on a rate-sensitive soil, it was essential to consider the effect of soil viscosity. Rowe and Hinchberger (1998) proposed an elasto-viscoplastic constitutive model and demonstrated

*Corresponding author. Tel.: +1 613 533 6933; fax: +1 613 533 6934.
E-mail address: kerry@civil.queensu.ca (R.K. Rowe).

0266-1144/$ - see front matter © 2007 Elsevier Ltd. All rights reserved.
doi:10.1016/j.geotexmem.2007.10.001

that the proposed model could adequately describe the behavior of the Sackville test embankment. Rowe and Li (2002) pointed out that the critical period with respect to the stability of reinforced embankments on rate-sensitive soils occurs after the end of construction as a result of a build-up in excess pore water pressure due to creep of the foundation soil. The installation of PVDs has the potential to minimize the effect of the delayed build-up in excess pore pressures on short-term embankment stability as illustrated by Rowe and Taechakumthorn (2007b). However, the effect of PVDs on the long-term performance of reinforced embankments on soft rate-sensitive soil has received very little attention in literature. Thus, the objective of this paper is to use the results of a finite element analysis validated for rate-sensitive soil (Rowe and Hinchberger, 1998; Hinchberger and Rowe, 1998) to provide insight regarding the combined effects of geosynthetics reinforcement and PVDs on both the short- and longer-term (i.e. to 98% degree of consolidation) behavior of embankments constructed on soft rate-sensitive soil. The effect of PVD spacing and other factors such as reinforcement stiffness, rate of construction and viscoplastic properties of soil will be examined. The time-dependent responses of excess pore water pressure, reinforcement strains, surface settlement and lateral deformation of the soil foundation are also investigated.

2. Finite element modeling and model parameters

2.1. Mesh discretization

A version of finite element program AFENA (Carter and Balaam, 1990) modified by Rowe and Hinchberger (1998) was adopted in this study to simulate the reinforced embankment construction. A series of small strain finite element analyses were conducted without updating of nodal coordinates. The drainage elements (Russell, 1990) implemented by Li and Rowe (2001) were utilized to study the effect of PVDs. The results presented here were obtained from embankments with 2H:1V side slopes overlaying 15 m of soft rate-sensitive clay deposit above the rigid and permeable layer. A typical finite element mesh (Fig. 1) involved 1815 six-noded triangle elements (4003 nodes) to discretize the embankment and foundation soils. Two-noded bar elements were used to model the reinforcement. Two-noded interface joint elements proposed by Rowe and Soderman (1985) were employed to model the fill/reinforcement and fill/foundation interfaces. The PVDs were modeled using two-noded drainage elements implemented by Li and Rowe (2001).

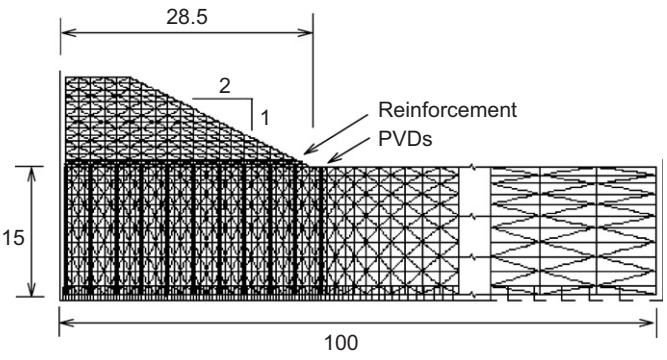

Fig. 1. Finite element mesh discretization.

The centerline of the embankment and far field boundary, located 100 m away from centerline, were taken to be smooth-rigid boundaries. The bottom boundary of mesh was assumed to be free drainage and rough-rigid. The embankment construction was simulated by gradually turning on the gravity of the embankment in 0.75 m thick lifts at a rate corresponding to the construction rate of the embankment. The PVDs were fully penetrating in a square pattern. The effect of the smear zone was considered in this study assuming that the ratio of equivalent radius of smear zone and vertical drains, s, was equal to 4. The details of PVDs and smear zone modeling are provided in Section 2.5.

2.2. Constitutive model for rate-sensitive soil and soil parameters

The elasto-viscoplastic model adopted herein (Rowe and Hinchberger, 1998) involves fully coupled deformation and consolidation (Biot, 1941) and incorporates Perzyna's theory of overstress viscoplasticity (Perzyna, 1963), an elliptical cap model (Chen and Mizuno, 1990), a Drucker–Prager failure envelope and concepts drawn from the critical state soil mechanics (Roscoe and Schofield, 1963). The constitutive model and computer program utilized in this study has been successfully verified with the results from the Sackville (Rowe and Hinchberger, 1998) and Gloucester (Hinchberger and Rowe, 1998) test embankments which were constructed on rate-sensitive soil. The main features of the model are summarized in this paper. Additional details regarding the model are provided by Hinchberger (1996) and Rowe and Hinchberger (1998).

The yield surface of the elliptical cap model in $\sigma'_m - \sqrt{2J_2}$ stress space (where σ'_m is mean effective stress and J_2 is second invariant of deviatoric stress tensor) is shown in Fig. 2. General equation of the elliptical cap model can be expressed as follows:

$$f = (\sigma'_m - l)^2 + 2J_2R^2 - (\sigma'_{my} - l)^2 = 0, \quad (1)$$

where l is the mean effective stress corresponding to the center of the ellipse, R is the ratio between major and minor axis of the ellipse and σ'_{my} is the intercept of the ellipse with the σ'_m axis.

The failure of the model is governed by the Drucker–Prager failure criterion having a slope of $M_{N/C}$ and $M_{O/C}$ for the normally consolidated and overconsolidated failure envelopes, respectively.

According to Pernazy's overstress theory, the governing equation is expressed in terms of strain rate tensor, $\dot{\varepsilon}_{ij}$ of

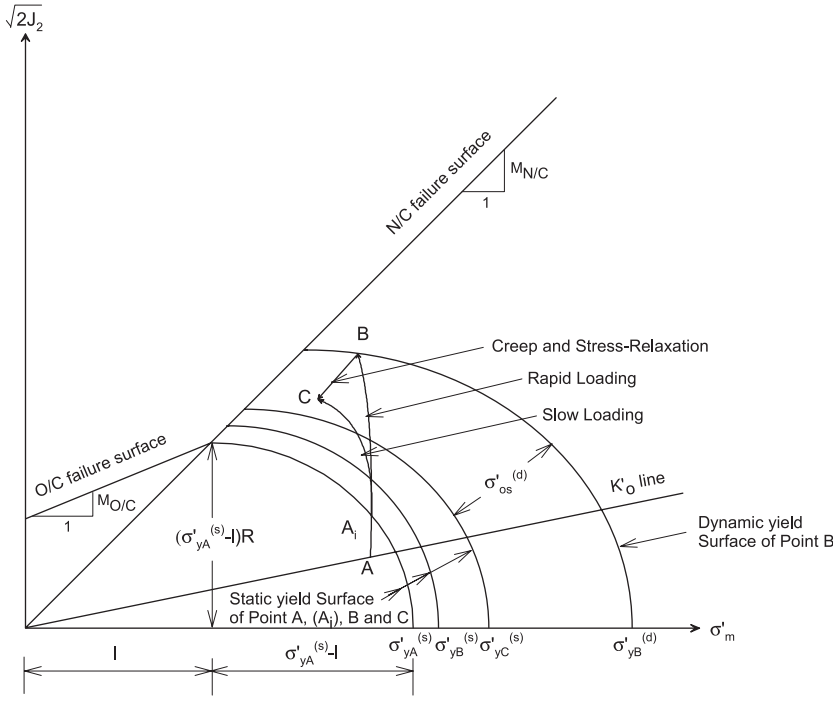

Fig. 2. Elliptical cap model (modified from Rowe and Hinchberger (1998)).

the elasto-viscoplastic materials:

$$\dot{\varepsilon}_{ij} = \frac{\dot{S}_{ij}}{2G} + \frac{1}{3K}\dot{\sigma}_{ii} + \gamma^{\mathrm{vp}}\langle\phi(F)\rangle\frac{\partial f}{\partial \sigma_{ij}}, \tag{2}$$

where S_{ij} is deviatoric stress, G is shear modulus, σ_{ii} is summation of the principle stresses, K is bulk modulus, γ^{vp} is the viscoplastic fluidity parameter and $\phi(F)$ is a flow function that can be expressed in terms of overstress as

$$\phi(F) = \left(\frac{\sigma'^{(\mathrm{s})}_{\mathrm{my}} + \sigma'^{(\mathrm{d})}_{\mathrm{os}}}{\sigma'^{(\mathrm{s})}_{\mathrm{my}}}\right)^{n} - 1, \tag{3}$$

where $\sigma'^{(\mathrm{d})}_{\mathrm{os}}$ is overstress, defined as the distance between dynamic and static yield surface at the current stress state as shown in Fig. 2 (Rowe and Hinchberger, 1998); n is strain rate exponent and f is plastic potential function. The elastic bulk modulus K and shear modulus G are a function of mean effective stress as shown below:

$$K = \frac{1+e}{\kappa}\sigma'_{\mathrm{m}}, \tag{4}$$

$$G = \frac{3(1-2v')K}{2(1+v')}, \tag{5}$$

where e is the void ratio, κ is the recompression index, σ'_{m} is mean effective stress and v is Poisson's ratio.

The basic constitutive parameters (Table 1) used for the soft rate-sensitive soil examined here are similar to those for the Sackville test embankment (Rowe and Hinchberger, 1998). The current states of stress were obtained from the preconsolidation and initial vertical stress profiles presented in Fig. 3.

Table 1
Foundation soil properties

Soil parameter	Soil CR1
Failure envelope, $M_{\mathrm{N/C}}$ (ϕ')	0.96 (29°)
Cohesion intercept, C_k (kPa)	0
Failure envelope, $M_{\mathrm{O/C}}$	0.75
Aspect ratio, R	1.25
Compression index, λ	0.16
Recompression index, κ	0.034
Coefficient of at rest earth pressure, K'_{o}	0.75
Poisson's ratio, v	0.3
Reference hydraulic conductivity, k_{vo} (m/s)	2×10^{-9}
Hydraulic conductivity ratio, $k_{\mathrm{h}}/k_{\mathrm{v}}$	4
Unit weight, γ (kN/m^3)	17
Initial void ratio, e_{o}	1.50
Viscoplastic fluidity, γ^{vp} (1/hour)	2.0×10^{-5}
Strain rate exponent, n	20

The hydraulic conductivity of soft clay was taken to be a function of void ratio as

$$k_{\mathrm{v}} = k_{\mathrm{vo}}\exp\left(\frac{e-e_{\mathrm{o}}}{C_{\mathrm{k}}}\right), \tag{6}$$

where k_{vo} is the reference hydraulic conductivity, e_{o} is the reference void ratio ($e_{\mathrm{o}} = 1.5$) and C_k is hydraulic conductivity change index ($C_k = 0.2$). The hydraulic

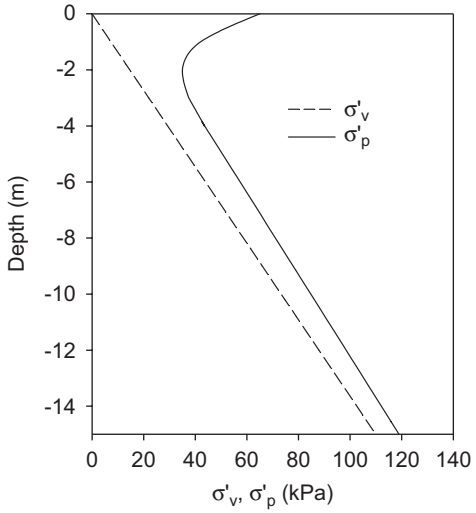

Fig. 3. Preconsolidation pressure and initial vertical stress profiles (based on Rowe and Li (2002)).

conductivity was considered to be anisotropic with $k_h/k_v = 4$.

2.3. Embankment fill parameters and construction rates

The purely frictional granular soil was used to model the embankment fill. The assumed properties were friction angle $\phi' = 37^\circ$, dilation angle $\psi = 6^\circ$ and unit weight $\gamma = 20\,\mathrm{kN/m^3}$. The non-linear elastic behavior of the fill was modeled using Janbu's (1963) equation

$$\frac{E}{P_a} = K\left(\frac{\sigma_3}{P_a}\right)^m, \tag{7}$$

where E is the Young's modulus, P_a is the atmospheric pressure, σ_3 is the minor principle stress and K and m are material constants selected to be 300 and 0.5, respectively. The construction rates of two cases examined in this study were 2, 4, 8, 6 and 10 m/month.

2.4. Interface parameters and reinforcement stiffness

The rigid–plastic joint elements (Rowe and Soderman, 1985) used to model the fill/reinforcement interfaces were assumed to be frictional with $\phi' = 37^\circ$. The axial tensile stiffness (J) of the bar elements used to model the reinforcement was varied with values of 0 (no reinforcement), 500, 1000, 2000, 4000 and 8000 kN/m being considered.

2.5. Drainage element and PVDs properties

Strictly speaking, the analysis of a system involving PVDs should be conducted using a full 3-D analysis. However, an appropriate approximation can be applied to consider vertical drains in a plane strain analysis. For instantaneous loading, Hansbo (1981) proposed that, for axisymmetric conditions, the average degree of consolidation on the horizontal plane (U_h) at depth z and time t as

$$U_h = 1 - \exp\left(\frac{-8T_h}{\mu}\right), \tag{8}$$

$$T_h = \frac{C_h t}{4R^2}, \tag{9}$$

$$\mu = \ln\left(\frac{n}{s}\right) + \left(\frac{k}{k_s}\right)\ln(s) - \frac{3}{4} + \pi z(2l - z)\frac{k}{q_w}, \tag{10}$$

$$n = \frac{R}{r_w}, \qquad s = \frac{r_s}{r_w} \quad \text{and} \quad q_w = \pi k_w r_w^2, \tag{11}$$

where T_h is the time factor for horizontal consolidation; C_h is the horizontal consolidation coefficient; k, k_s and k_w are the hydraulic conductivities of soil in the horizontal direction, soil in the smear zone (the hydraulic conductivity of soil in smear zone was assumed to be isotropic and same as vertical hydraulic conductivity) and the vertical drain, respectively; q_w is the equivalent discharge capacity for the axisymmetric unit cell; r_w, r_s and R are the radius of the vertical drain, smear zone and influence zone, respectively, and l is the drainage length of vertical drains. In plane strain conditions, Hird et al. (1992) showed that T_h and μ can be expressed as follows:

$$T_h = \frac{C_h t}{4B^2} \quad \text{and} \quad \mu = \frac{2}{3} + 2z(2l - z)\frac{k}{BQ_w}, \tag{12}$$

where B and Q_w are the half width of the spacing in plane strain conditions and the equivalent discharge capacity for the plane strain unit cell. To match the average degree of consolidation at any time and depth in these two conditions, the average degree of consolidation in the horizontal plane for axisymmetric conditions can simply be set to be equal to that for plane strain condition as

$$U_h^{pl} = U_h^{ax}. \tag{13}$$

This can be achieved by geometric matching, permeability matching or a mix of geometric and permeability matching. In previous work by Li and Rowe (2001), the permeability matching scheme was adopted. To satisfy Eq. (13), the hydraulic conductivity of soil and equivalent discharge capacity of vertical drains in plane strain analysis have to be modified to

$$k_{pl} = \frac{2k_{ax}}{3[\ln(n/s) + (k_{ax}/k_s)\ln(s) - 3/4]} \quad \text{and} \quad Q_w = \left(\frac{2}{\pi R}\right)q_w, \tag{14}$$

where k_{pl} and k_{ax} are horizontal hydraulic conductivities of soil in plane strain and axisymmetric conditions, respectively. Details of the drainage element implemented in this study are provided in Li and Rowe (2001).

2.6. PVDs properties

The PVDs in this study were modeled to have typical rectangular cross-section of 100 mm × 4 mm (Holtz, 1987) that was equivalent to a 52 mm diameter (d_w) circular drain, based on Rixner et al. (1986): $d_w = (b+t)/2$, where b and t are the width and thickness of the drains, respectively. The PVDs spacing (S) of 1, 2 and 3 examined are within the typical range used in practice (Holtz, 1987). The discharge capacity of PVDs was taken to be 100 m^3/year (Rixner et al., 1986) unless otherwise noted.

3. Results and discussions

To examine the short-term responses, reinforced embankments were numerically constructed at the different construction rates examined until failure. To examine the long-term behavior, the reinforced embankments were constructed up to the 5 m height and numerically monitored with time. Time-dependent variation in mobilized reinforcement strain, excess pore pressures and foundation deformations were investigated.

3.1. Short-term stability of reinforced embankments

The short-term stability of an embankment can be assessed in terms of failure height of the embankment. The failure height of either a reinforced and an unreinforced embankment can be defined as the height of fill at which any attempt to increase the fill materials will not result in an increase in the net embankment height (actual height above the original ground surface). This failure height was obtained by plotting the relationship between the net embankment heights (fill thickness minus settlement) against the fill thickness as presented in Fig. 4. The results from rate-insensitive soil or non-viscous soil (NV), shown in Fig. 4, were simulated using the conventional elasto-plastic constitutive model discounting the effect of soil viscosity while the others were obtained using the elasto-viscoplastic constitutive model. The viscosity of soil prevents the plastic deformation during the initial stage of loading and provides the extra short-term strength to the soil. The short-term failure height of Cases I and II were 4.0 and 6.6 m, respectively. For rate-sensitive soil, the faster the loading rate, the stronger the short-term strength of the soil. The results from Cases II and III in Fig. 4 demonstrate the effect of construction rate as the short-term failure height for Case III was 7.2 m, 9.1% higher than that for Case II.

For the case of unreinforced embankment, the lateral thrust from fill material is directly transferred to the foundation; however, when reinforcement is present some of the lateral thrust is carried by the reinforcement, thus improving the bearing capacity of the foundation. The role of the geosynthetics reinforcement in improving the short-term stability of the reinforced embankments is illustrated in Fig. 5. Reinforced embankments with reinforcement stiffness of 0 (unreinforced), 500 and 1000 kN/m were constructed with different construction rates until failure. The stiffer reinforcement provides higher confining force to the system and that results in higher bearing capacity of the foundation soil and therefore a higher short-term failure height. Fig. 5 also illustrates the effect of construction rate on the short-term failure height of the embankment as the faster construction rate resulted in higher short-term failure height.

Even though the faster construction rate allows the mobilization of higher short-term strength and hence a greater failure height, the consequent larger overstress in the system can be expected to result in the development of larger post-construction excess pore water pressures and strength loss with time that may result in post-construction failure. The presence of PVDs provides a short horizontal drainage path for soft clay and takes advantage of any higher horizontal hydraulic conductivity to accelerate the dissipation of the excess pore water pressures in the soil.

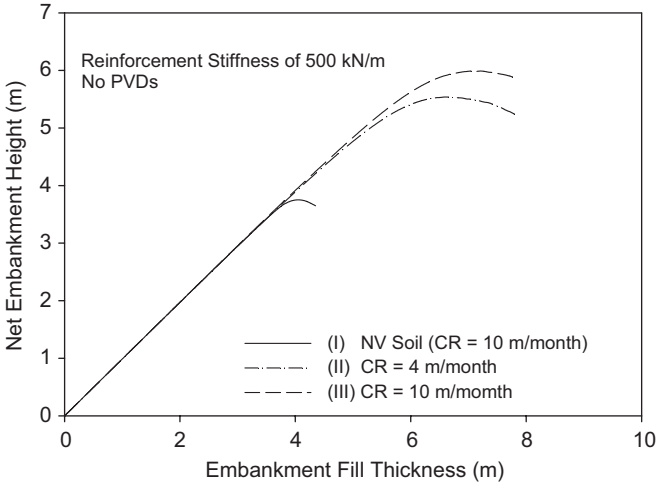

Fig. 4. Effects of rate-sensitivity and construction rate on the short-term embankment failure height.

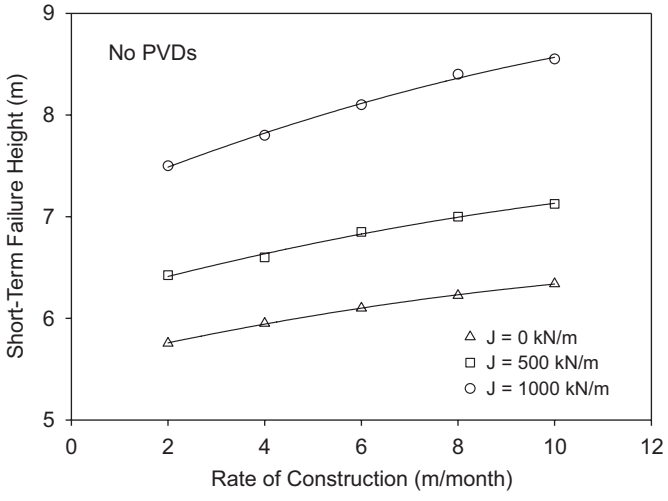

Fig. 5. Effects of reinforcement stiffness and construction rate on the short-term embankment failure height.

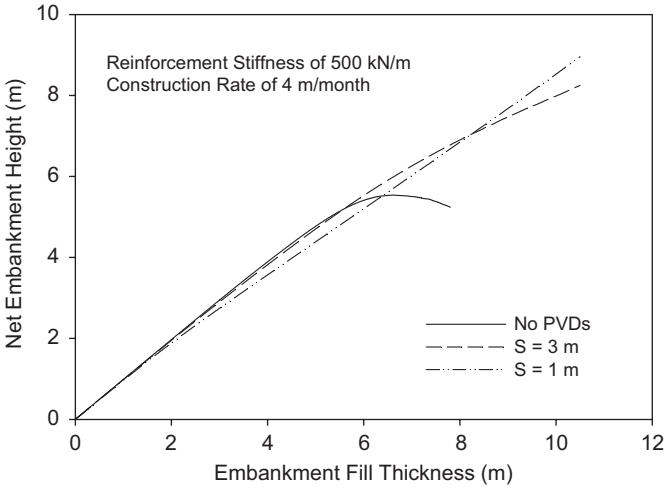

Fig. 6. Effect of PVDs on short-term embankment failure height.

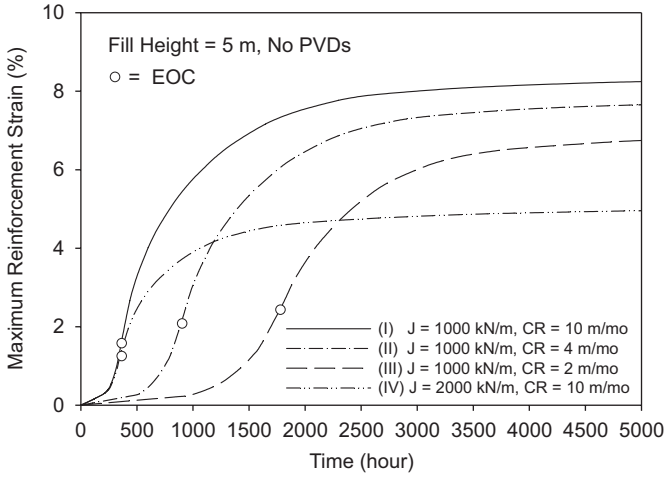

Fig. 7. Effects of construction rate and reinforcement stiffness on the maximum mobilized reinforcement strain with time.

This can be expected to increase the rate of strength gain due to the consolidation, reduce the amount of overstress and minimize the effect of time-dependent viscoplastic responses such as creep and stress relaxation in the soil.

The benefit of PVDs on the short-term stability is illustrated in Fig. 6. The short-term failure height of a reinforced embankment with the reinforcement stiffness of 500 kN/m and no PVDs (Case I) was 5.8 m. When PVDs were employed, the short-term stability of the reinforced embankment was improved substantially and there was no failure even when the fill was built up to 10.5 m. During the initial stage of construction, the smaller PVD spacing ($S = 1$ m) gave larger settlement due to the higher degree of partial consolidation. However, the higher degree of partial consolidation resulted in smaller overstress in the soil and accordingly less viscoplastic deformation was generated. Thus for $S = 1$ m, after the fill thickness exceeded 8.5 m, the net embankment height exceeded that for $S = 3$ m.

3.2. The effects on the long-term reinforcement strain

As noted above, the greater overstress associated with the ability to construct higher embankments on a rate-sensitive foundation than over an otherwise similar (e.g. same slow strain undrained strength) but not rate-sensitive soil can be expected to cause longer-term problems for reinforced embankments. To illustrate this, a conventional preliminary design was conducted using the limit equilibrium analysis and a shear strength profile for the soft deposit calculated based on the results of plane strain shear strength test with the recommended strain rate of 0.5–1.0%/h (Germaine and Ladd, 1988). The analysis implied that the 5.25 m height reinforced embankment should be stable with safety factors of 1.3 using reinforcing tensile force of 100 kN/m (e.g. $J = 2000$ kN/m at 5% strain). However, the results from finite element analysis show that for this case, the long-term reinforcement strain was 6%, which implies that the stability calculated from limit equilibrium analysis is over-estimated. For this particular soil, a reinforced embankment (with $J = 2000$ kN/m) could be constructed to only 5 m in order to limit the long-term reinforcement strain within allowable design strain of 5%.

The effects of construction rate and reinforcement stiffness on the long-term mobilized reinforcement strains are illustrated in Fig. 7. At the end of construction, soil in Case I (faster construction rate) exhibited higher short-term strength and since the soil carried most of the load from the embankment, the reinforcement only had a small maximum mobilized strain of 1.6%. In contrast, the slower construction rates, while giving higher end of construction strains (2.1% and 2.6% for Cases II and III, respectively, compared to 1.6% for Case I), allowed higher degree of consolidation during the construction and reduced the amount of overstress in the soil. This reduced the consequences creep and delayed excess pore pressures (as discussed later in this paper) and hence resulted in smaller (7.7% and 6.7% for Cases II and III, respectively) long-term strains than the 8.3% obtained for Case I. The results from Cases I and IV show the effect of reinforcement stiffness and as expected, the stiffer reinforcement (Case IV) gave both a smaller strains at both the end of construction and long-term (1.3% and 5.0%, respectively) than those for Case I (1.6% and 8.3%).

The presence of PVDs not only accelerated the rate of excess pore water dissipation but also reduced the amount of overstress in the soil, consequently the effects of viscoplastic response of the soil was minimized. For a 5 m high reinforced embankment with the reinforcement stiffness $J = 1000$ kN/m, even a construction rate as low as 2 m/month gave rise to a long-term reinforcement strain of 6.8% which exceeds the typical allowable limit of 5% (Fig. 7). In contrast, with PVDs at 3 m spacing, when the same embankment was numerically constructed at 10 m/month, it still only gave a maximum long-term reinforcement strain of 4.8% (Case I—with resistance,

Fig. 8). With stiffer ($J = 2000$ kN/m) reinforcement, PVDs reduced the long-term reinforcement strain from 5.0% to 3.4% (Case IV in Fig. 7 and Case II—with resistance, Fig. 8). With a reinforcement stiffness of 2000 kN/m, a reinforced embankment could be constructed up to 5.75 m without the long-term reinforcement strain exceeding about 5.2% (Case III—with resistance, Fig. 8). For this same 5% long-term limit strain and PVDs at 3 m spacing, embankments could be constructed to 6.50 and 7.85 m compared to 5.80 and 7.10 m (without PVDs) for $J = 4000$ and 8000 kN/m, respectively.

The "with resistance" analyzes reported above were performed assuming that the PVDs had a maximum discharge capacity of 100 m^3/year. To assess the effect of this restriction, analyzes were also performed for the case where the PVDs were "free draining" (i.e. there was no resistance to flow once water reached the PVDs) and these results are also presented in Fig. 8. The "free draining" analyzes result in lower predicted strains than those with resistance. This is because the free draining case gave rise to a higher degree of partial consolidation and less overstress was generated in the soil. Consequently, the amount of viscoplastic strain in the foundation was under predicted.

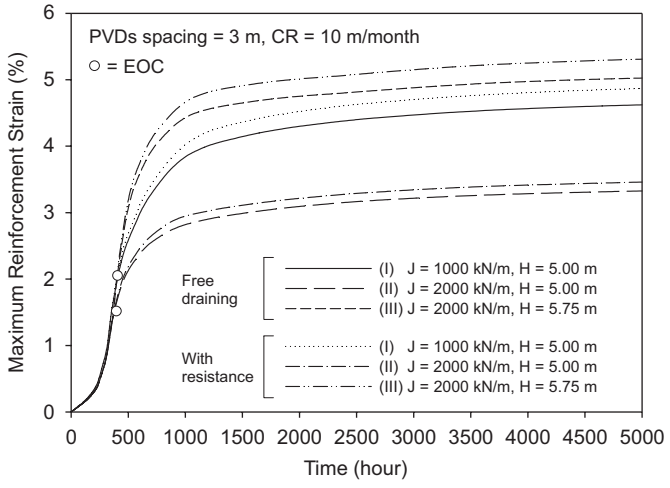

Fig. 8. Effects of PVDs and reinforcement stiffness on the mobilization of reinforcement strain with time.

3.3. The effects on the excess pore water dissipation

Following the construction of reinforced embankments on a rate-sensitive soil, there is simultaneous generation of excess pore water pressure due to creep of overstressed soil and dissipation of excess pore pressures due to consolidation. Fig. 9 shows the contours of the excess pore water pressure for a 5 m high reinforced embankment ($J = 2000$ kN/m), at 1 month after the end of construction. The shear-induced nature of much of the excess pore pressure is evident from the fact that the maximum excess pore water was developed along the potential failure zone and not beneath the centerline as might be expected on a more traditional (inviscous) soil. The contours of the change in excess pore water pressure between immediately after and 1 month after the end of construction (Fig. 10) illustrate this point while also showing how creep-induced excess pore water pressures are generated post-construction even when pore pressure dissipation is occurring. Thus, the maximum excess pore water pressure and the minimum factor of safety were reached following the end of construction.

The effect of reinforcement stiffness and PVDs on the excess pore water pressure is presented in Fig. 11. The excess pore water pressures were monitored at 6.0 m beneath the crest of the embankment where the maximum increase in excess pore water pressure was indicated (Fig. 10). The results show that the excess pore water pressures at the end of construction were approximately 80 kPa for all cases regardless of reinforcement stiffness for the construction rate of 10 m/month. The excess pore water pressures kept increasing post-construction for all reinforcement stiffnesses considered until a peak was reached. This phenomenon is similar to that observed at the Sackville test embankment (Rowe and Hinchberger, 1998).

The installation of PVDs significantly minimized the effect of delayed excess pore water pressure build-up on the

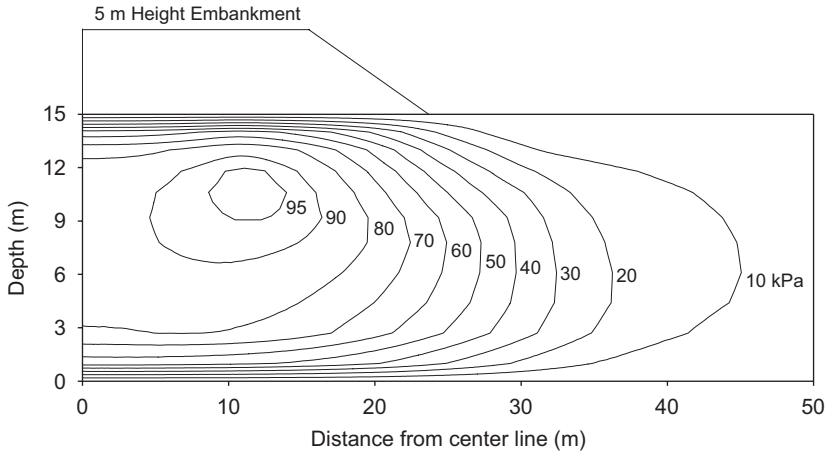

Fig. 9. Contours of excess pore water pressures 1 month after the end of construction (CR = 10 m/month, $J = 2000$ kN/m).

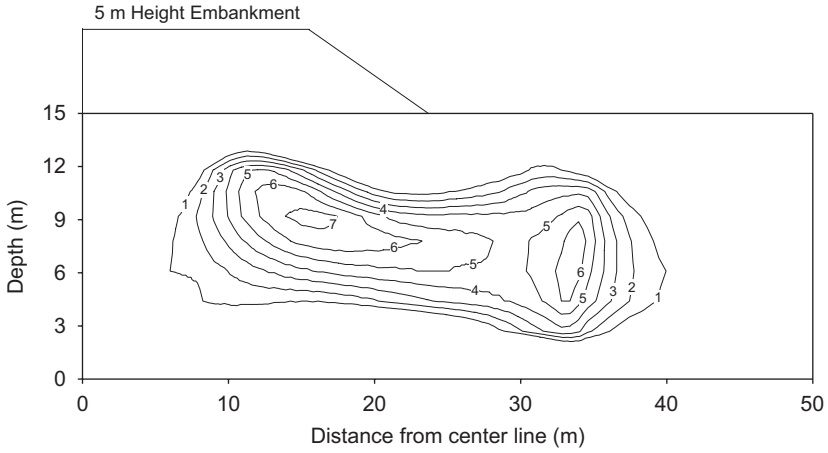

Fig. 10. The difference of excess pore water contour at the end of construction and 1 month after the end of construction (CR = 10 m/month, $J = 2000$ kN/m).

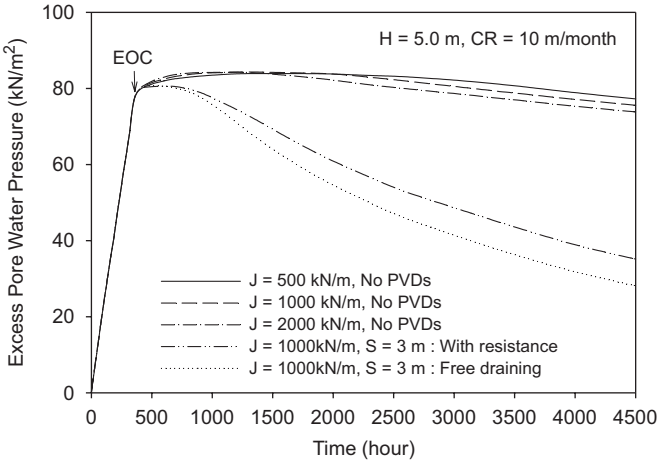

Fig. 11. Effect of reinforcement stiffness and PVDs on the dissipation of excess pore pressure with time at the location of the maximum difference shown in Fig. 10 (i.e. 6 m beneath the embankment shoulder).

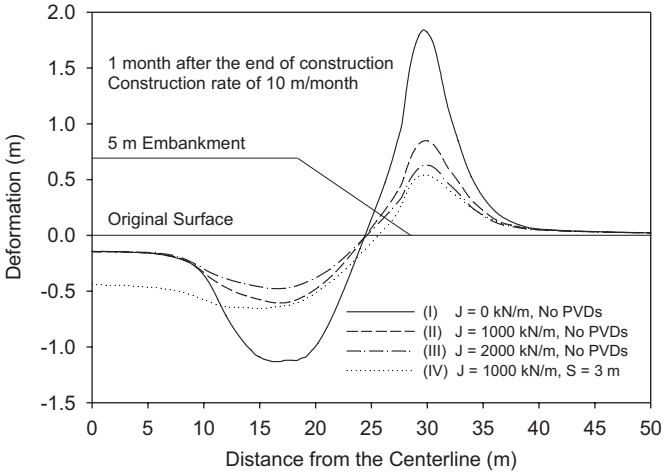

Fig. 12. Effect of reinforcement stiffness and PVDs on the differential settlement of the foundation surface.

rate-sensitive soil. The results show that with PVDs, the excess pore water pressure rapidly decreased following the end of construction and reinforcement with lesser stiffness could be employed with faster rate of construction while maintaining similar performance. As mentioned earlier, the analyzes for free draining PVDs over-estimated the degree of partial consolidation compared to the analyzes that took account of flow resistance in the PVDs. To demonstrate the effect of the assumption about flow resistance in the PVD on pore pressures, Fig. 11 shows the calculated variation in excess pore water pressure with time for the two assumed conditions.

3.4. The effects on the differential settlement and lateral deformation of the embankment

Reinforcement can significantly reduce differential settlement, heave and lateral deformations of the embankment on rate-sensitive soil. Fig. 12 shows the ground surface profiles for embankments with different reinforcement stiffnesses at 1 month after the end of construction. For the case of an unreinforced embankment ($J = 0$ kN/m), the differential settlement between center and crest of the embankment was almost 1.2 m but for the reinforced embankments, this was reduced to 0.47 and 0.34 m for reinforcement stiffness of 1000 and 2000 kN/m (Cases II and III), respectively. The maximum calculated heaves were 1.8, 0.85 and 0.63 m for the unreinforced embankment and for the reinforcement stiffness of 1000 and 2000 kN/m, respectively. The presence of PVDs considerably reduced the differential settlement of the foundation soil. The result from Case IV shows that for $J = 1000$ kN/m, installation of PVDs with spacing of 3 m resulted in larger settlement beneath the centerline of the embankment (0.45 m versus 0.14 m for no PVD) due to a higher degree of partial consolidation. However, the differential settlement and maximum heave were reduced to 0.15 and 0.54 m, respectively (compared to 0.34 and 0.63 m for Case III with $J = 2000$ kN/m), even with less stiff reinforcement ($J = 1000$ kN/m).

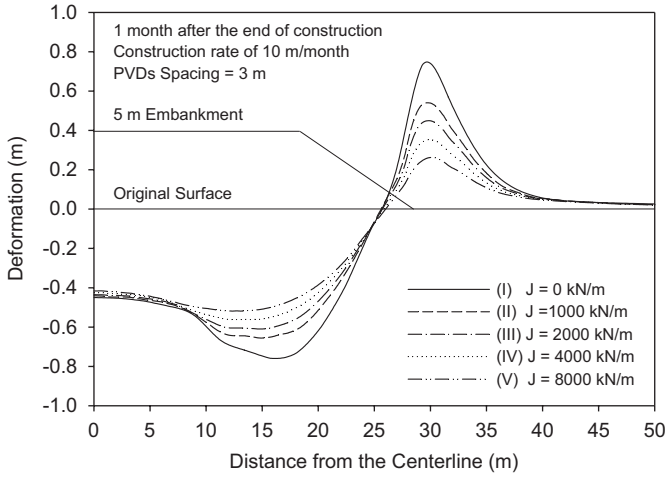

Fig. 13. Effect of reinforcement stiffness on the differential settlement of the foundation (PVDs at 3 m spacing for all cases).

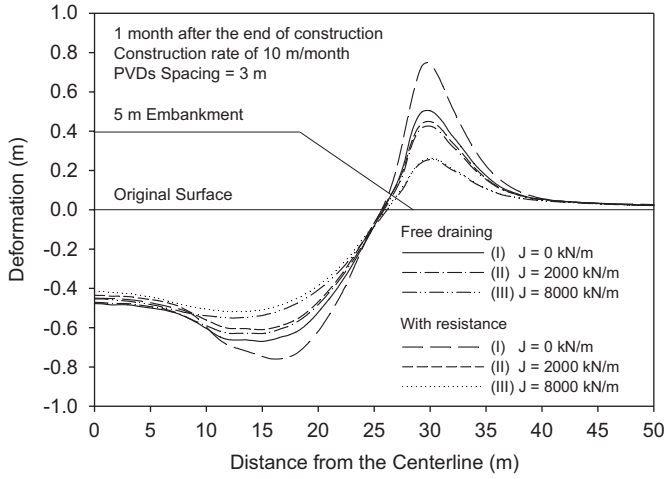

Fig. 14. Effect of assumptions regarding resistance to drainage in the PVDs on the differential settlement at the foundation surface.

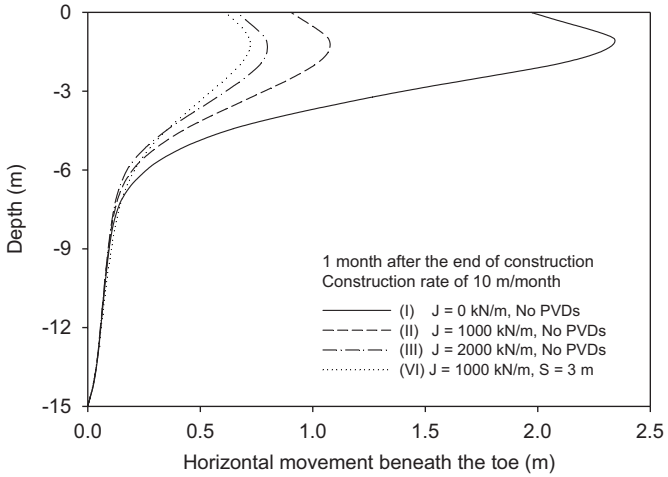

Fig. 15. Effect of reinforcement stiffness and PVDs on the horizontal deformation beneath the embankment toe.

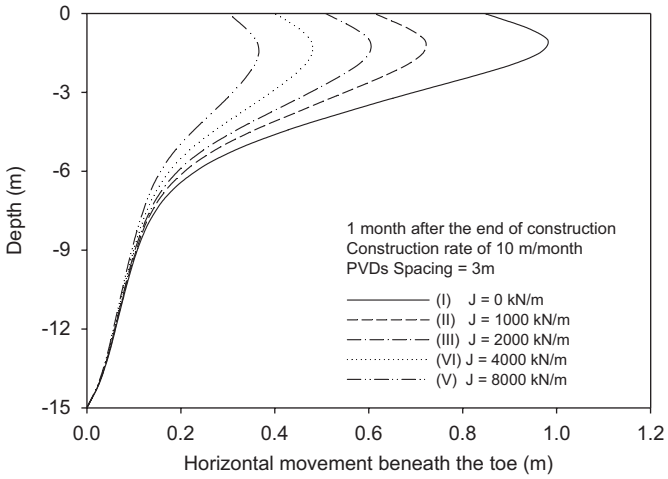

Fig. 16. Effect of reinforcement stiffness on horizontal deformation beneath the embankment toe (PVDs at 3 m spacing for all cases).

The combined effect of reinforcement and PVDs on the differential settlement is illustrated in Fig. 13. The stiffer reinforcement resulted in less differential settlement as well as less heave. Fig. 14 shows the effect of assumption regarding drainage resistance on the calculated differential settlement. For the case of unreinforced embankment, the differential settlement between center and crest of the embankment and maximum heave for free draining PVDs (Case I—free draining) were 0.19 and 0.48 m, respectively, as compared to 0.26 and 0.74 m when the resistance of the PVDs was considered (Case I—with resistance). Thus, the free draining case may result in unconservative predictions of differential settlement for the unreinforced embankment. In contrast, the assumption regarding drainage in the PVDs had very little effect on the predicted differential settlement for the two reinforced embankments (Cases II and III).

Reinforcement also has a benefit in reducing the lateral deformation of the foundation soil. Fig. 15 shows the profile of horizontal deformation beneath the toe of the reinforced embankment at 1 month after the end of construction. Without reinforcement, there was excessive movement beneath the toe of the embankment and eventually failure. The maximum lateral deformations of soil were reduced from 2.4 m, for the unreinforced case, to 1.1 and 0.78 m for reinforcement stiffness of 1000 and 2000 kN/m, respectively. Fig. 15 also shows the effect of PVDs on the lateral deformation. With a reinforcement stiffness of 1000 kN/m and PVDs with spacing of 3 m, the maximum lateral deformation was only 0.61 m.

The combined effect of reinforcement and PVDs on the lateral deformation is also presented in Fig. 16. The effect of reinforcement on lateral deformation was more pronounced than that on differential settlement when the PVDs were employed. As expected, the stiffer the reinforcement, the smaller is the maximum lateral deformation. For this particular soil installed with PVDs with spacing of 3 m, the maximum lateral deformations were

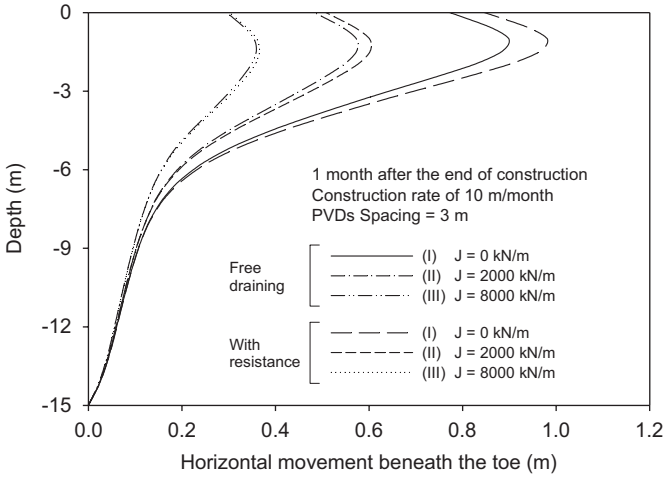

Fig. 17. Effect of assumptions regarding resistance to drainage in the PVDs on horizontal deformations beneath the embankment toe.

0.98, 0.72, 0.60, 0.48 and 0.37 for the case of reinforcement stiffness of 0, 1000, 2000, 4000 and 8000 kN/m, respectively.

The effect of assumption regarding drainage resistance in the PVDs on the lateral deformation is shown in Fig. 17. The effect was similar to that for differential settlement with the free draining PVD analyzes under-predicting the later deformation of the foundation. The presence of reinforcement in the system can reduce the effect of assumptions regarding flow resistance in the PVD.

4. Summary and conclusions

The time-dependent behavior of reinforced embankments constructed over rate-sensitive clay with and without PVDs was investigated using finite element analysis. Various factors such as the viscoplastic properties of the foundation soil, reinforcement stiffness, construction rate and PVDs spacing were examined. The results show that the viscoplastic behavior of the foundation soil can have a significant effect on the performance of a reinforced embankment, especially after the end of construction. The behavior of reinforced embankment on the specific rate-sensitive clays, within the range of cases and parameters considered in this paper, can be summarized as follows.

For the rate-sensitive soil, the short-term stability was affected by viscoplastic characteristics of the soil. Other things being equal, a faster construction rate gave higher strength and hence a higher short-term failure height; but field experiences shows that failure can occur some time after the construction. Reinforcement and PVDs both significantly increased the short-term stability of the embankment. The construction rate affected the long-term reinforcement strains since, the faster construction rate resulted in higher short-term strength of the foundation soil; therefore, less force was transferred to the reinforcement and a smaller reinforcement strain was mobilized at the end of construction. However, a faster construction rate gave higher overstress in the foundation soil and that lead to larger creep deformation in soil as well as larger long-term reinforcement strain. Most of the time, the height of the reinforcement embankment is limited by the allowable reinforcement strain. With the combined use of PVDs and reinforcement, less stiff reinforcement was required in the design for the same embankment height compared to when there were no PVDs. Alternatively with PVDs, a higher embankment height could be achieved if same stiffness of reinforcement was employed.

Without PVDs, the excess pore water pressures reached the maximum value after the end of construction. Thus, the critical period regarding the stability for the embankment (the time of minimum factor of safety) may occur after the end of construction. Although this maximum excess pore pressure was not very sensitive to the reinforcement stiffness, the pore pressures dissipated faster for the more highly reinforced embankment. PVDs accelerated the excess pore water pressure dissipation and largely eliminated post-construction build-up in excess pore water pressure. The differential settlement, heave and lateral deformation were all substantially reduced by the use of basal reinforcement and the effect could be enhanced using PVDs.

The assumptions made regarding flow resistance in the PVDs had a notable effect of predicated settlement and horizontal deformations for the unreinforced embankments modeled. The effect was much less significant for the reinforced embankments examined; however, even in these cases it seems appropriate to model the expected flow resistance in the PVDs since the assumption of free draining PVDs may result in unconservative predictions of both deformations and reinforcement strains.

Acknowledgment

The research reported in this paper was supported by the Natural Sciences and Engineering Research Council of Canada (NSERC).

References

Bergado, D.T., Teerawattanasuk, C., 2008. 2D and 3D numerical simulations of reinforced embankments on soft ground. Geotextiles and Geomembranes, in press, doi:10.1016/j.geotexmem.2007.03.003.

Bergado, D.T., Balasubramaniam, A.S., Fannin, R.J., Holtz, R.D., 2002a. Prefabricated vertical drains (PVDs) in soft Bangkok clay: a case study of the new Bangkok International Airport project. Canadian Geotechnical Journal 39, 304–315.

Bergado, D.T., Long, P.V., Murthy, B.R., 2002b. A case study of geotextile-reinforced embankment on soft ground. Geotextile and Geomembranes 20, 343–365.

Biot, M.A., 1941. General theory of three-dimensional consolidation. Journal of Applied Physics 12, 155–164.

Bo, M.W., 2004. Discharge capacity of prefabricated vertical drain and their field measurements. Geotextiles and Geomembranes 22 (1/2), 37–48 (Special issue on Prefabricated Vertical Drains).

Carter, J.P., Balaam, N.P., 1990. AFENA—A General Finite Element Algorithm: Users Manual. School of Civil Engineering and Mining Engineering, University of Sydney, NSW 2006, Australia.

Chai, J.C., Miura, N., 1999. Investigation of factors affecting vertical drain behaviour. Journal of Geotechnical and Geoenvironmental Engineering 125 (3), 216–226.

Chai, J.C., Miura, N., Nomura, T., 2004. Effect of hydraulic radius on long-term drainage capacity of geosynthetics drains. Geotextiles and Geomembranes 22 (1/2), 3–16 (Special issue on Prefabricated Vertical Drains).

Chai, J.C., Carter, J.P., Hayashi, S., 2006. Vacuum consolidation and its combination with embankment loading. Canadian Geotechnical Journal 43, 985–996.

Chen, W.F., Mizuno, E., 1990. Nonlinear Analysis in Soil Mechanics: Theory and Implementation. Elsevier Science Publishing Company Inc., New York, USA.

Crawford, C.B., Fannin, R.J., deBoer, L.J., Kern, C.B., 1992. Experiences with prefabricated vertical (wick) drains at Vernon, B.C. Canadian Geotechnical Journal 29, 67–79.

Fowler, J., Koerner, R.M., 1987. Stabilization of very soft soils using geosynthetics. In: Proceedings of the Geosynthetics '87 Conference, New Orleans, vol.1, pp. 289–299.

Germaine, J.T., Ladd, C.C., 1988. Triaxial testing of saturated cohesive soils. Advanced Triaxial Testing of Soil and Rock. ASTM STP 977, pp. 421–459.

Graham, J., Crooks, H.A., Bell, A.L., 1983. Time effects on the stress–strain behaviour of natural soft clays. Geotechnique 33, 327–340.

Hansbo, S., 1981. Consolidation of fine-grained soils by prefabricated drains. In: Proceedings of the 10th International Conference on Soil Mechanics and Foundation Engineering, Stockholm, vol. 3, pp. 677–682.

Hinchberger, S.D., 1996. The behaviour of reinforced and unreinforced embankments on soft rate-sensitive foundation soils. Ph.D. Thesis. Department of Civil Engineering, The University of Western Ontario, London, Ont.

Hinchberger, S.D., Rowe, R.K., 1998. Modelling the rate-sensitive characteristics of the Gloucester foundation soil. Canadian Geotechnical Journal 35, 769–789.

Hird, C.C., Pyrah, I.C., Russell, D., 1992. Finite element method modelling of vertical drains beneath embankment on soft ground. Geotechnique 42 (3), 499–511.

Holtz, R.D., 1987. Preloading with prefabricated vertical strip drains. Geotextiles and Geomembranes 6 (1–3), 109–131.

Indraratna, B., Redana, I.W., 2000. Numerical modeling of vertical drains with smear and well resistance installed in soft clay. Canadian Geotechnical Journal 37, 132–145.

Janbu, N., 1963. Soil compressibility as determined by oedometer and triaxial tests. In: Proceedings of the European Conference on Soil Mechanics and Foundation Engineering, Wiesbaden, Germany, vol. 1, pp. 19–25.

Jewell, R.A., 1987. Reinforced soil walls analysis and behaviour. In: Jarret, P.M., McGown, A. (Eds.), The Application of Polymeric Reinforcement in Soil Retaining Structures. Kluwer Academic Publishers, pp. 365–408.

Kabbaj, M., Tavenas, F., Leroueil, S., 1988. In situ and laboratory stress–strain relationships. Geotechnique 38 (1), 83–100.

Kelln, C., Sharma, J., Hughes, D., Gallagher, G., 2007. Deformation of a soft estuarine deposit under a geotextile reinforced embankment. Canadian Geotechnical Journal 44, 603–617.

Leroueil, S., 1988. Tenth Canadian geotechnical colloquium: recent developments in consolidation of natural clays. Canadian Geotechnical Journal 25, 85–107.

Li, A.L., Rowe, R.K., 1999. Reinforced embankments constructed on foundations with prefabricated vertical drains. In: Proceedings of the 52nd Canadian Geotechnical Conference, Regina, Sask, pp. 411–418.

Li, A.L., Rowe, R.K., 2001. Combined effects of reinforcement and prefabricated vertical drains on embankment performance. Canadian Geotechnical Journal 38, 1266–1282.

Lo, K.Y., Morin, J.P., 1972. Strength anisotropy and time effects of two sensitive clays. Canadian Geotechnical Journal 9 (3), 261–277.

Nagahara, H., Fujiyama, T., Ishiguro, T., Ohta, H., 2004. FEM analysis of high airport embankment with horizontal drains. Geotextiles and Geomembranes 22 (1–2), 49–62 (Special issue on Prefabricated Vertical Drains).

Perzyna, P., 1963. The constitutive equations for rate-sensitive plastic materials. Quarterly of Applied Mathematics 20 (4), 321–332.

Rixner, J.J., Kraemer, S.R., Smith, A.D., 1986. Prefabricated vertical drains. Engineering Guidelines, FWHA/RD-86/168, vol. I. Federal Highway Administration, Washington, DC.

Roscoe, K.H., Schofield, A.N., 1963. Mechanical behaviour of an idealised "wet clay". In: Proceedings of the Second European Conference on Soil Mechanics, pp. 47–54.

Rowe, R.K., 1984. Reinforced embankments: analysis and design. Journal of Geotechnical Engineering, ASCE 110 (GT2), 231–246.

Rowe, R.K., Hinchberger, S.D., 1998. The significance of rate effects in modelling the Sackville test embankment. Canadian Geotechnical Journal 33, 500–516.

Rowe, R.K., Li, A.L., 1999. Reinforced embankments over soft foundations under undrained and partially drained conditions. Geotextiles and Geomembranes 17 (3), 129–146.

Rowe, R.K., Li, A.L., 2002. Behaviour of reinforced embankments on soft rate sensitive soils. Geotechnique 52 (1), 29–40.

Rowe, R.K., Soderman, K.L., 1985. An approximate method for estimating the stability for geotextiles reinforced embankments. Canadian Geotechnical Journal 22 (3), 392–398.

Rowe, R.K., Soderman, K.L., 1987. Reinforcement of the embankments on soils whose strength increase with depth. In: Proceedings of Geosynthetics '87 Conference, New Orleans, vol.1, pp. 266–277.

Rowe, R.K., Taechakumthorn, C., 2007a. Behaviour of reinforced embankments on soft rate-sensitive foundations. In: Proceedings of Geosynthetics Conference 2007, Washington DC, USA, pp. 86–98

Rowe, R.K., Taechakumthorn, C., 2007b. The counteracting effects of rate of construction on reinforced embankments on rate-sensitive clay. In: Proceedings of the 5th International Conference on Earth Reinforcements IS Kyushu 2007, Kyushu, Japan, in press.

Rowe, R.K., Gnanendran, C.T., Landva, A.O., Valsangkar, A.J., 1995. Construction and performance of a full-scale geotextile reinforced test embankment, Sackville, New Brunswick. Canadian Geotechnical Journal 32 (3), 512–534.

Rowe, R.K., Gnanendran, C.T., Landva, A.O., Valsangkar, A.J., 1996. Calculated and observed behaviour of a reinforced embankment over soft compressible soil. Canadian Geotechnical Journal 33, 324–338.

Rujikiatkamjorn, C., Indraratna, B., Chu, J., 2007. Numerical modelling of soft soil stabilized by vertical drains, combining surcharge and vacuum preloading for a storage yard. Canadian Geotechnical Journal 44, 326–342.

Russell, D., 1990. An element to model thin, highly permeable materials in two dimensional finite element consolidation analyses. In: Proceedings of the 2nd European Specialty Conference on Numerical Method in Geotechnical Engineering, Santander, Spain, pp. 303–310.

Shen, S.L., Chai, J.C., Hong, Z.S., Cai, F.-X., 2005. Analysis of field performance of embankments on soft clay deposit with and without PVD-improvement. Geotextiles and Geomembranes 23 (6), 463–485.

Sinha, A.K., Havanagi, V.G., Mathur, S., 2007. Inflection point method for predicting settlement of PVD improved soft clay under embankments. Geotextiles and Geomembranes 25 (6), 336–345.

Vaid, Y.P., Campanella, G., 1977. Time-dependent behaviour of undisturbed clay. Journal of the Geotechnical Engineering 103 (GT7), 693–709.

Vaid, Y.P., Robertson, P.K., Campanella, R.G., 1979. Strain rate behaviour of Saint-Jean-Vianney clay. Canadian Geotechnical Journal 16, 34–42.

Varuso, R.J., Grieshaber, J.B., Nataraj, M.S., 2005. Geosynthetic reinforced levee test section on soft normally consolidated clays. Geotextiles and Geomembranes 23 (4), 362–383.

Zhu, G., Yin, J.H., 2001. Design charts for vertical drains considering construction time. Canadian Geotechnical Journal 38 (5), 1142–1148.

Zhu, G., Yin, J.H., 2004. Consolidation analysis of soil with vertical and horizontal drainage under ramp loading considering smear effects. Geotextiles and Geomembranes 22 (1/2), 63–74.